Simulation of turbulent flows around a prism in suburban terrain inflow based on random flow generation method

Yi-Chao Li[1*)], Chii-Ming Cheng[2)], De-qian Zheng[3)], Yuan-Lung Lo[2)], Fuh-Min Fang[4)] ,Chia-Kuo Wang[2)]

1) Wind Engineering Research Center, Tamkang University, New Taipei City, Taiwan
2)Department of Civil Engineering, Tamkang University, New Taipei City, Taiwan
3) School of Civil Engineering and Architecture, He'nan University of Technology, Zhengzhou, China
4) Department of Civil Engineering, National Chung Hsing University, Taichung, Taiwan
**) presenting author, liyichao223@gmail.com*

ABSTRACT

In this study, the modified discretizing and synthesizing random flow generation (MDSRFG) was adopted to generate an anisotropic boundary layer inlet for Large-eddy simulation. The statistical quantities including mean velocity, turbulence intensity, and turbulence length scale of inlet were defined by the measurements of suburban terrain at TKU BL-1 wind tunnel. The target spectra were also defined by von Kármán models. Results showed that the turbulence energy can be maintained from the inlet to the downstream position. Comparison of aerodynamic coefficient between simulation and experiments yielded consistent results. A square pressure model with aspect ratio h/D=3 was established for validation. The mean and fluctuating pressure distributions of simulation also showed good agreements with experiments. The result indicated that adopting a reasonable process in the MDSRFG method can be an effective numerical tool for generating a spatially correlated atmospheric boundary layer flow field.

1 INTRODUCTION

The aerodynamic behaviour of the prism in the atmospheric boundary layer has been a typical problem in wind engineering. An appropriate turbulence inlet can not only maintain the mean wind speed and the turbulence characteristics to the downstream, but also generate reliable wind force on structures. Therefore, simulation of a suitable atmospheric boundary layer inlet is one of the most important works of the computational techniques. To successfully validate this technique, The discretizing and synthesizing random flow generation (DSRFG) method, a improving inflow turbulence generation method developed by Huang et al. (2010), is adopted to produce an inlet fluctuating velocity field that meet specific spectrum. Castro et al. (2011) modified the DSRFG to MDSRFG by preserving the statistical quantities at the inlet part of the computation domain and keeping independence of number of points for simulating target spectrum. However, few studies investigated and successfully maintained statistical quantities of the turbulence boundary layer from inlet to the downstream of computation domain. There are still some technical and theoretical problems need to be overcome.

Thus, this paper attempts to generate the suburban terrain inlet by MDSRFG. Parameters, such as mean wind speed, turbulence intensity, turbulence integral scale, and power spectra from suburban turbulent boundary layer flow are provided from TKU BL-1 wind tunnel tests. A pressure prism model with aspect ratio h/D=3 is established in a suburban terrain to validate the numerical results.

2 METHOD

2.1 Wind tunnel experiment

In order to assure the reliability of the turbulence boundary inlet based on MDSRFG for Large-eddy simulation, a square pressure model is built and tested in a wind tunnel with test section of 17m(L) × 2m(W) ×1.5m(H). The turbulent boundary layer flow, designated by suburban terrain with power law index α= 0.25 is generated to represent wind profiles over suburban terrain. The free stream velocity of approach flow is 8.85 m/s. The corresponding Reynolds number is 7.5×10^5 by the definition in terms of $U_\delta D/\nu$. The aspect ratio of square pressure model is 3. The sampling rate is 200Hz and the sample length is 287 seconds.

Figure 1: Photograph of pressure model in TKU BL-1 with suburban terrain

2.2 Numerical method

In the weakly-compressible-flow method (Song, 1988), the continuity and momentum equations are

$$\frac{\partial p}{\partial t}+\nabla\cdot\left(k\vec{V}\right)=0 \tag{1}$$

$$\frac{\partial \vec{V}}{\partial t}+\vec{V}\cdot\nabla\vec{V}=-\nabla\frac{p}{\rho}+\nabla\cdot\left[(\nu+\nu_t)\nabla\vec{V}\right] \tag{2}$$

where p, $\vec{V}$ and t denote respectively pressure, velocity and time; k is the bulk modulus of elasticity of air; ν and ν_t are respectively the laminar and turbulent viscosities. The turbulent viscosity (ν_t) is determined based on a subgrid-scale turbulence model as

$$\nu_t=C_S\Delta^2\left(\frac{S_{ij}^2}{2}\right)^{0.5} \tag{3}$$

where C_S is the Smagorinsky coefficient; Δ denotes the characteristic length of the computational grid and $S_{ij}=(\partial u_j/\partial x_i+\partial u_i/\partial x_j)$. Based on a concept of dynamic model proposed by Germano *et al*. (1991), two grid systems, corresponding respectively to a grid filter and a test filter, are used in the flow calculations. By comparing the resulting differential turbulent shear stresses associated with the two filter systems at a certain time step in the computation, the C_S value at the next time step is then obtained.

A finite-volume method is adopted to calculate and then update the fluxes within each elapsed time based on an explicit predictor-corrector scheme (MacCormack, 1969). During the computation process, the time increment is limited by the CFL criterion (Courant et al., 1967).

2.3 Synthesizing method

Derivation of the MDSRFG method and associated validation researches are given by Castro et al. (2011). A brief formulation of the method is presented as below.

$$U(x,t)=\sum_{m=1}^{M}\sum_{n=1}^{N}\left[p_i^{m,n}\cos\left(\tilde{k}_j^{m,n}\tilde{x}_j+\omega_{m,n}\frac{t}{\tau_0}\right)+q_i^{m,n}\sin\left(\tilde{k}_j^{m,n}\tilde{x}_j+\omega_{m,n}\frac{t}{\tau_0}\right)\right] \tag{4}$$

where

$$p_i^{m,n}=sign\left(r_i^{m,n}\right)\sqrt{\frac{4c_i}{N}E_i(k_m)\Delta k_m\frac{\left(r_i^{m,n}\right)^2}{1+\left(r_i^{m,n}\right)^2}} \tag{5}$$

$$q_i^{m,n}=sign\left(r_i^{m,n}\right)\sqrt{\frac{4c_i}{N}E_i(k_m)\Delta k_m\frac{1}{1+\left(r_i^{m,n}\right)^2}} \tag{6}$$

with $\omega_{m,n}\in N(0,2\pi f_m)$, $r_i^{m,n}$ is a three dimensional normal distributed random number with $\mu_r=0$ and $\sigma_r=0$. $c_i=0.5\overline{U}$ and $\overline{U}$ is the mean wind speed. $\tilde{x}=x/L_s$ and $L_s=\theta_1\sqrt{L_u^2+L_v^2+L_w^2}$ is the scaling factor for spatial correlation. $\tau_0=\theta_2 L_s/\overline{U}$ is a parameter introduced to allow some control over the time correlation. The turbulence kinematic energy $\tilde{k}^{m,n}=\mathbf{k}^{m,n}/k_0$ is the three dimensional distribution on the sphere of inhomogeneous and anisotropic turbulence.

The auto-correlation function can be computed by some mathematical manipulation form equation (4):

$$\overline{u(x,t)u(x,t+\tau)}=\frac{2c}{N}\sum_{m=1}^{M}\sum_{n=1}^{N}E(k_m)\Delta k_m\cos\left(\frac{\tau}{\tau_0}\omega_{m,n}\right) \tag{7}$$

The auto-correlation coefficients are dominated by frequency segments (Δk_m) and time correlation parameter θ_2. An expression for the spatial correlation can be obtained in an analogous way:

$$\overline{u(x,t)u(x',t)}=\sum_{m=1}^{M}\sum_{n=1}^{N}\frac{2}{N}E(k_m)\cos\left[\tilde{k}_j^{m,n}\frac{(x'_j-x_j)}{L_s}\right] \tag{8}$$

Both of the above equation shows that the spatial correlation and auto-correlation are controlled by L_s, and are used in the same spectrum $E(k_m)$.

2.4 Computation domain and meshes

The simulation domain for the present study is 33D in the along-wind (X) direction (-5< x/D < 28), 16D in the across-wind (Y) direction, and 10D in the vertical direction, where D represents the width of the prism model. In this study, two typical cases are established, which are the empty test section (without the prism) and a prism with h/D=3 setting at x/D=4. In both the cases, 3-D computations are performed in the study. Figure 2 shows the computation domain and the corresponding mesh system (251×101×101).

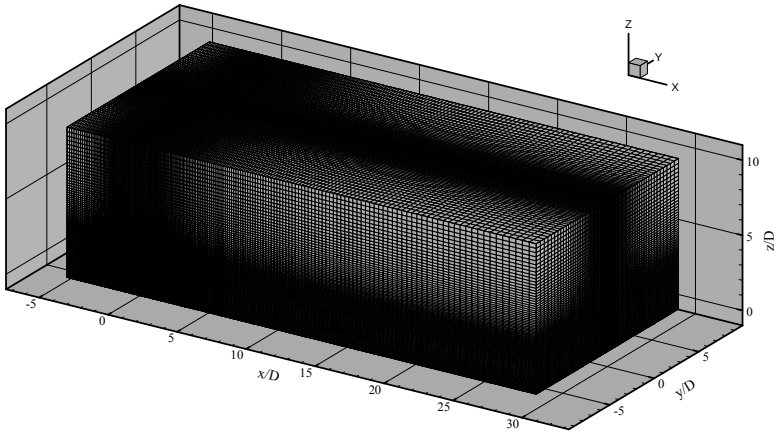

Figure 2: Computation domain and grid system

2.5 Boundary conditions

Appropriate values of pressures and velocities are specified at exterior cells (or phantom cells) to reflect the correct physical nature of the boundaries. The ground and the prism surface condition is assumed no-slip. The top, both sides and downstream boundaries are assumed zero-gradient conditions (in the directions normal to the boundaries).

The upstream boundary condition is generated by the MDSRFG method. The inhomogeneous anisotropic turbulent conditions of the suburban terrain field are created in this study. Basically, the experimental spectra of the three principal velocity components are consistent with von Kármán models, defined as

$$\text{u-component: } S_u(f) = \frac{4\left(I_u\overline{U}\right)^2\left(L_u/\overline{U}\right)}{\left[1+70.8\left(fL_u/\overline{U}\right)^2\right]^{5/6}} \tag{9}$$

$$\text{v-component: } S_v(f) = \frac{4\left(I_v\overline{U}\right)^2\left(L_v/\overline{U}\right)\left[1+188.4\left(2fL_v/\overline{U}\right)^2\right]}{\left[1+70.8\left(2fL_v/\overline{U}\right)^2\right]^{11/6}} \tag{10}$$

$$\text{w-component: } S_w(f) = \frac{4\left(I_w\overline{U}\right)^2\left(L_w/\overline{U}\right)\left[1+188.4\left(2fL_w/\overline{U}\right)^2\right]}{\left[1+70.8\left(2fL_w/\overline{U}\right)^2\right]^{11/6}} \tag{11}$$

All the given parameters are obtained from TKU BL1 wind tunnel experiments. The mean wind speed profile is set to follow the power law with α=0.25. The longitudinal turbulence intensity profile is set to $I_u = 0.3 - 0.26(z/\delta)^{0.35}$. The longitudinal length scale (L_u) profile is regressed to a polynomial of degree 6, Because of the lack of v- and w-component of turbulence intensity and length scale, the assumption of the turbulence intensity is adopted in the other two directions, as $I_v = 0.75I_u$ and $I_w = 0.5I_u$ respectively. L_v and L_w are both assumed as $0.5L_u$. The experimental, curve-fitted and assumed of results are shown in Figure 3.

Before synthesizing the wind speed of inlet, an important work is the definition of spatial parameter θ_1 and time parameter θ_2. From equation (7), θ_2 is a parameter introduced to allow some control over the auto-correlation, therefore θ_2 can adjust the turbulence integral length scale to correspond original setup.

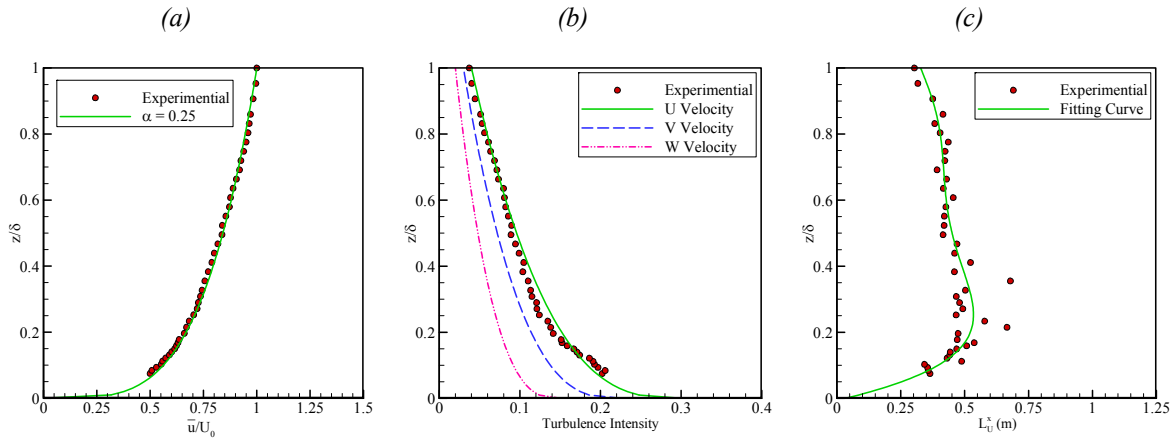

Figure 3: Vertical profiles of Inlet condition (a) mean wind speed, (b) turbulence intensity and (c) integral length scale.

Equation (8) gives a convenient way to estimate the spatial correlation between the synthesizing points having the same spectra as each other. Actually, the turbulence boundary layer spectra significantly vary along the vertical direction. In order to define the spatial correlation for determining θ_1, a theoretical equation for reference, the square root of coherence (also known as narrow-band cross-correlation) proposed by Davenport (1968), is adopted to be the target spectra:

$$Coh = e^{-\hat{f}},\ \hat{f} = \frac{n\left[C_z^2(z_1 - z_2)^2 + C_y^2(y_1 - y_2)^2\right]^{1/2}}{0.5\left[U(z_1) + U(z_2)\right]} \tag{12}$$

where y_1, y_2, z_1, z_2 are the coordinate on y-z plane. C_y and C_z are the exponential decay coefficient in the horizontal and vertical direction respectively. $C_z = 10$ and $C_y = 16$ are suggested by Davenport(1968), which consist with the results of TKU BL1 suburban terrain. In the boundary layer flow field, the main variation of turbulence intensity and turbulence integral length scale profile are all along the vertical direction, therefore the adjustment of θ_1 is based on fitting the vertical coherences to correspond the theoretical function. Figure 4 show the coherence values of varying with horizontal and vertical positions when =5.5. The simulation patterns are close to target spectra. Hence, the spatial correlation results from simulation with θ_1=5.5 are consistent with theoretical curves.

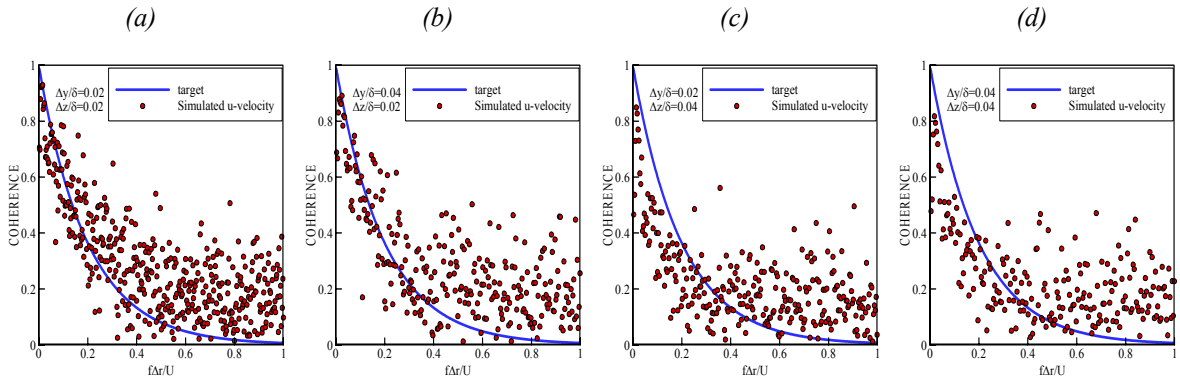

Figure 4. Cross coherence at z/δ=0.5 with θ_1=5.5 (a) Δy/δ=0.02 Δz/δ=0.02, (b) Δy/δ=0.04 Δz/δ=0.02, (c) Δy/δ=0.02 Δz/δ=0.04, (d) Δy/δ=0.04 Δz/δ=0.04.

3 RESULTS

3.1 Velocity profiles and spectra

To survey the suburban terrain inlet generating by the MDSRFG, conducting the adjusting process in section 2.4, is of an empty test section first. The turbulence flow field is generated by MDSRFG with sampling frequency, say 200Hz. The total generating times and simulating times both are 120 seconds.

Figure 5(a) shows the mean wind speed profile maintain fairly well form the upstream boundary to x/D=10, and corresponding to the target obeying the power law with α=0.25. The turbulence intensity profiles in 3 components from inlet to the downstream (x/D=10) are depicted in figure 4(b) to figure 4(d), respectively. The I_u profile generated by the MDSRFG (x/D=0) has well agreement with the target as assumptions in section 2.5. The u-component turbulence still maintain the main energy even x/D=10. Although the I_v profile at inlet (x/D=0) has slightly over-prediction between z/δ=0.05 to 0.2, but the other profiles are self-mixed by the sub-grid turbulent to correspond the target profile. The I_v profiles have consistent with target, but a slight decay happens near the ground. Because of the symmetric boundary condition is used on the top surface of domain, all of the turbulence intensity profiles have little overestimate near z/δ=1 in the computation domain. The phenomenon should be improved by extending the computation of vertical direction.

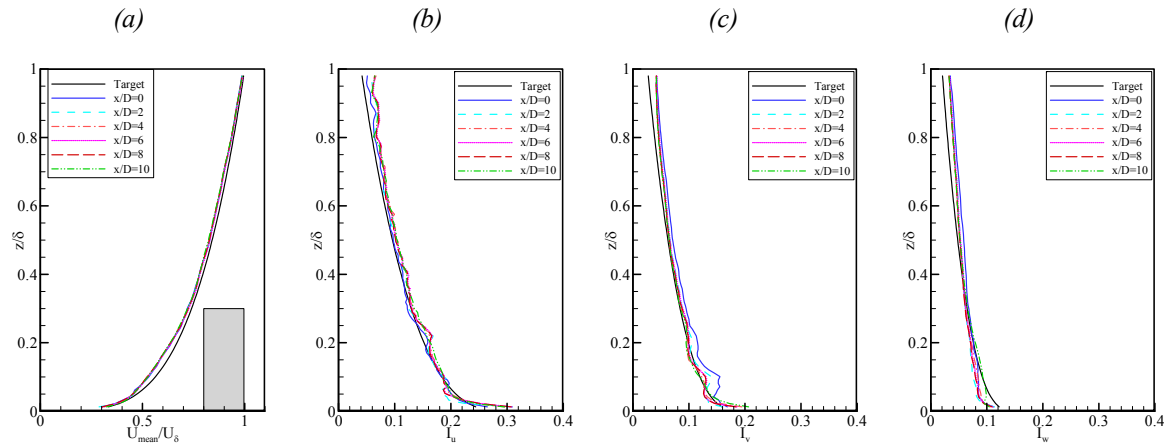

Figure 4: Comparison of mean velocity and turbulence intensity from inlet to x/D=10 with target profiles. (a) mean wind speed, (b) turbulence intensity of u-component, (c) turbulence intensity of v-component, (d) turbulence intensity of u-component.

The results of three components power spectra in three heights (z/δ= 0.25, 0.75, 0.5) and four positions (x/D= 0, 2, 4, 6) are shown in Figure 5. The trends of inlet spectra (x/D=0) consist with the target spectra. The spectra of u-component correspond to target spectra in computation domain (x/D=2, 4, 6). The v- and w-components spectra have well agreement with target basically, but the energy starting decay about at the dimensionless frequency $fL_x/U=1$. This might be due to the assumption of length scale profiles of u- and v-components are not well enough to maintain the energy of small scale eddy. Fortunately, the turbulence energy losses of the two components are minor, and the preservation of turbulence energy in u-component is the major control of the wind load on the prism.

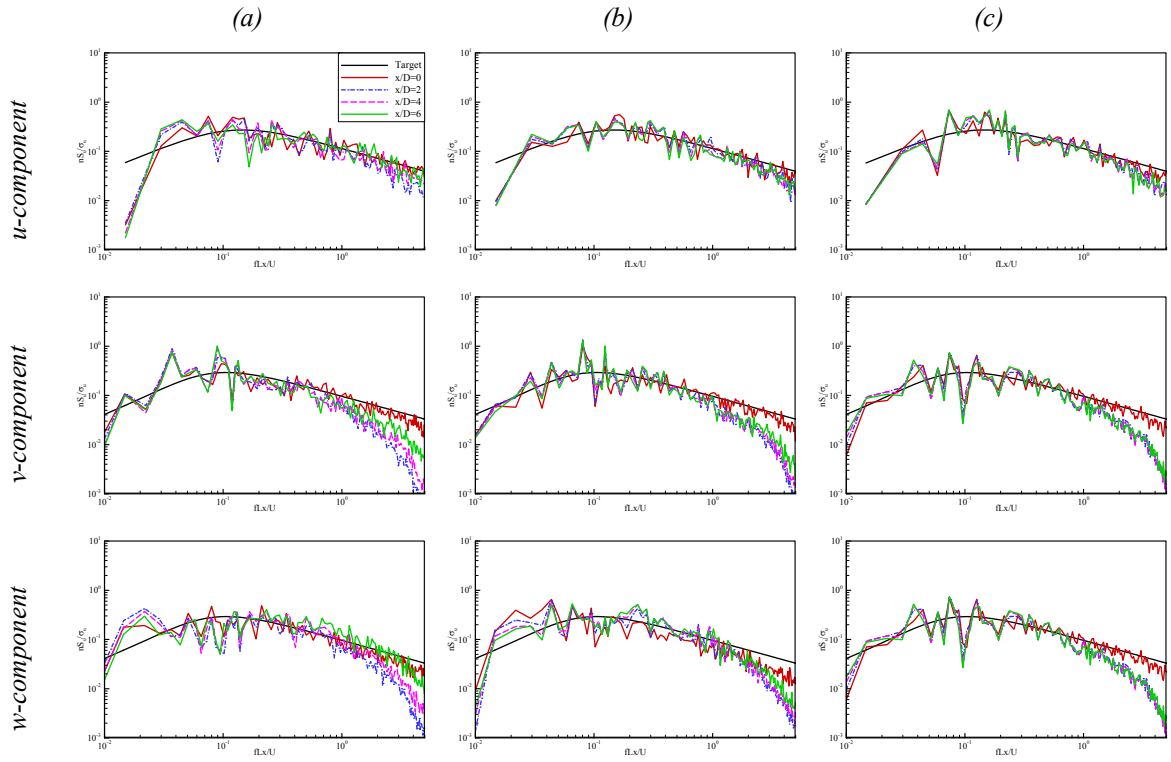

Figure 5: Comparison of the 3-components power spectra. (a) z/ δ=0.25, (b) z/ δ=0.5 and (c) z/ δ=0.75.

3.2 Aerodynamic characteristic

Table 1 lists the comparison results of the mean drag coefficient ($\overline{C_D} = \overline{F_x}/0.5\rho U_h^2 DH$), fluctuating drag coefficient ($C_D' = F_x'/0.5\rho U_h^2 DH$), fluctuating lift coefficient ($C_L' = F_y'/0.5\rho U_h^2 DH$) and Strouhal number ($n_{peak}\mathrm{D}/U_h$) of the prism with the experiments. $\overline{C_D}$ and Strouhal number are close to the experimental results, expect 3-5% over-prediction over here**.** The fluctuating values of simulation are small than experiments. There are about 20-24 % under-prediction of $C_D^{'}$ and $C_L^{'}$.

Table 1: Comparisons of Aerodynamic coefficients

	$\overline{C_D}$	$C_D^{'}$	$C_L^{'}$	Strouhal Number
Experimental	0.853	0.228	0.203	0.085
Numerical	0.882	0.183	0.151	0.089

Figure 6 compares the results of the mean coefficients ($\overline{C_p} = \bar{p}/0.5\rho U_h^2$) and the fluctuating pressure coefficients ($C_p' = p'/0.5\rho U_h^2$) on the prism at y/D=0 between the experiments. The simulating results of $\overline{C_p}$ on the windward and the leeward of the prism are approximately close to the experimental results. C_p' by simulating on windward essential correspond to the experimental results, but slightly overestimate near the top of the prism. The overestimating values of C_p' also happens on leeward. The values of error are about 3-23 %. The reason of the overestimate might cause by the stronger turbulence eddy energy in simulation.

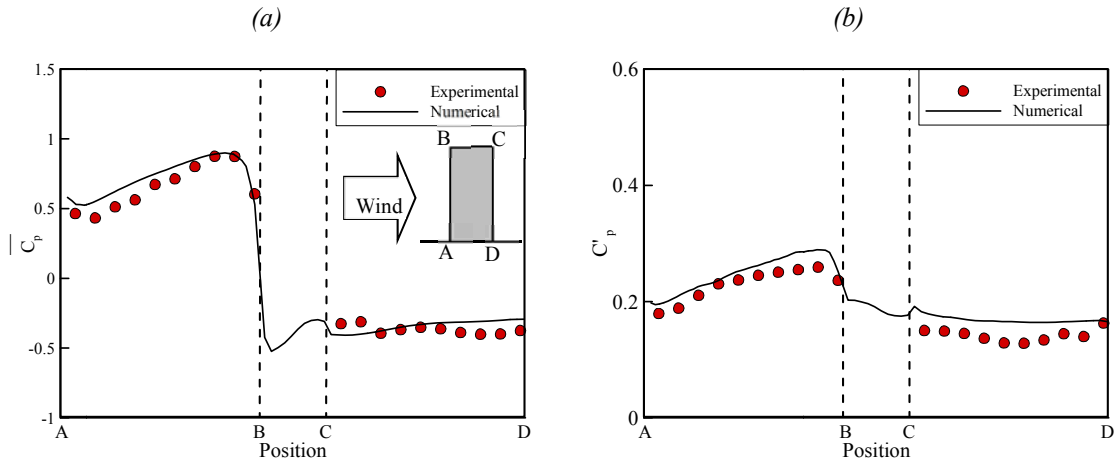

Figure 6: Comparisons of surface pressure on the prism

4 CONCLUSIONS

In this research, the MDSRFG is adopted to generate the inlet boundary condition of the suburban terrain flow field for Large-Eddy simulation. The mean wind speed profile, turbulence intensity profile and power spectra of velocity fluctuations of simulation results fit fairly well to targets, these results are consistent with those Castro (2011). The results indicate that the most of the eddy turbulence energy maintain quite well even to the downstream. The viewpoint also is supported by the results of the pressure coefficient on the prism. The parameters of spatial and time correlations are adjusted by wind tunnel results and theoretical equations to prove that the MDSRFG method is an effective numerical tool for generating a spatially correlated atmospheric boundary layer flow field. This process might extend to generate different terrains for further research.

References

Huang, S. H., Li, Q. S. and Wu, J. R. (2010), "A General Inflow Turbulence Generator for Large Eddy Simulation, " Journal of Wind Engineering and Industrial Aerodynamic, Vol.98, 600-617.

Castro, H. G., Paz, R. R., and Sonzogni, V. E. (2011), "Generation of Turbulence Inlet Velocity Conditions for Large Eddy Simulation," Mecánica Computational, Vol. XXX, 2275–2288.

Li, Y. C., Cheng, C. M., Fang, F. M., Chang, C. H. and Lo, Y.L., (2013), "Generation of Suburban Terrain Inflow Conditions for Large Eddy Simulations", The Eighth Asia-Pacific Conference on Wind Engineering, Chennai, India.

Song, C., Yuan, M. (1988), "A weakly compressible flow model and rapid convergence methods," Journal of Fluids Engineering, 110(4), 441-455.

Germano, M., Piomelli, U. Moin, P. and Cabot, W.H. (1991). "A dynamic subgrid-scale eddy viscosity model," Physics of Fluids, **3**, 1760-1765.

MacCormack, R. (1969), "The effect of viscosity in hyper-velocity impact cratering," AIAA paper 69-354.

Smagorinsky, J., 1963. General circulation experiments with primitive equations. Month Weather Review 91(3), 99-164.

Courant, R. Friedrichs, K.O. and Lewy, H.(1967), "On the partial difference equations of mathematical physics," IBM Journal, **11**, 215-234.

Davenport, A. G. (1968), "The dependence of wind load upon Meteorological Parameter," in Proceedings of the International Research Seminar on Wind Effects on Buildings and Structures, University of Toronto Press, Toronto, pp. 19-82.